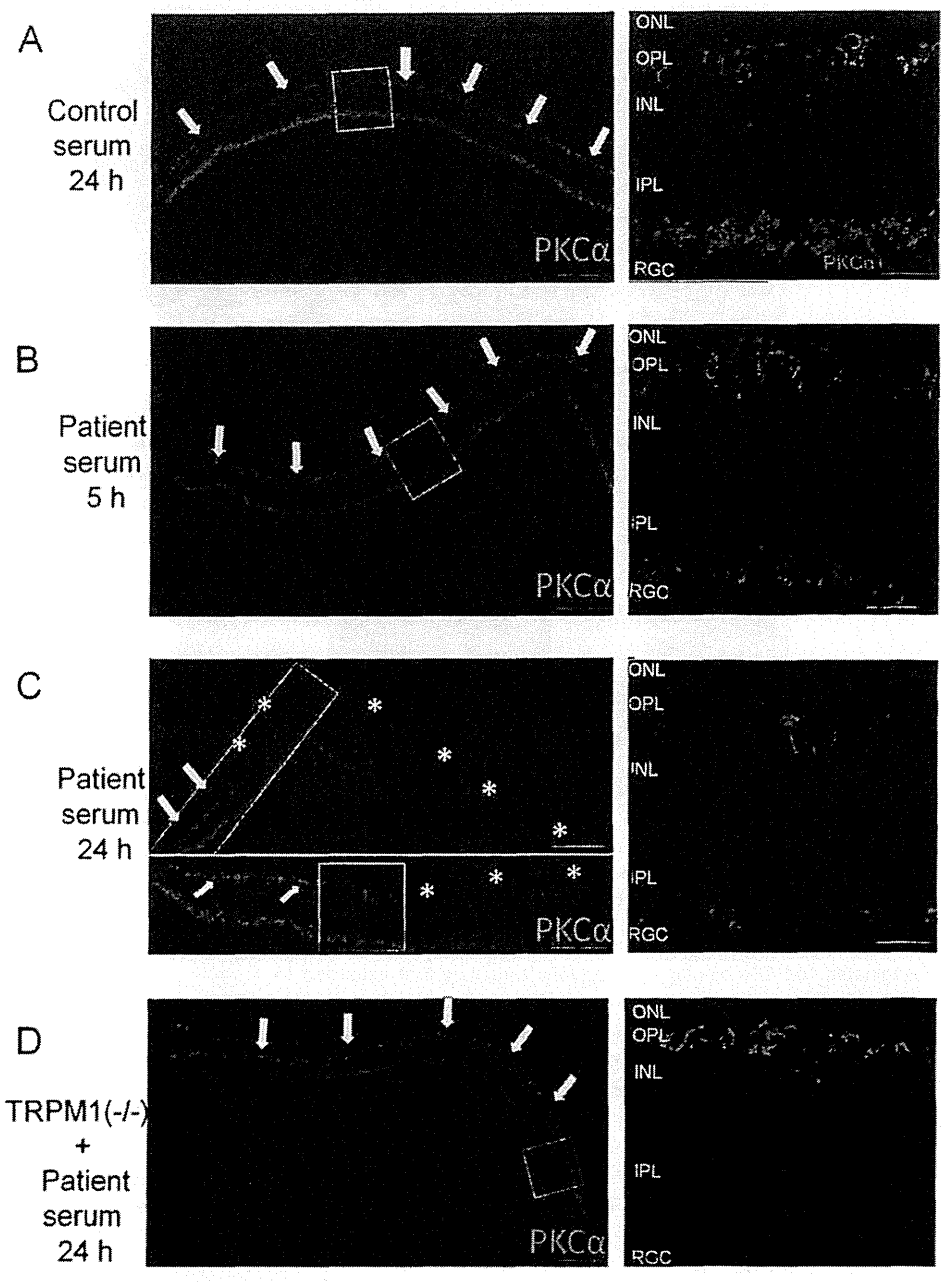

Figure 4. Distribution of ON bipolar cell marker (PKCα) in the retina after serum injection. Wild type mouse retina 24 hours after control serum injection (A) and wild type mouse retina 5 hours (B) and 24 hours (C) after intravitreal injection with the patient's serum. Retina from TRPM1 knockout mouse 24 hours after intravitreal injection with the patient's serum.(D) Mouse retinas were stained with anti PKCα antibody (green) and co-stained with DAPI (blue) in the high magnification micrographs (A-C, right). Photomicrographs of the regions outlined by the white boxes are enlarged either to the right or the below the original images. The peripheral retina is oriented to the left and the central retina to the right. PKCα staining can be seen in the entire retina at both 5 hours after the patient serum injection and 24 hours after control serum injection (A and B, arrows). But the PKCα staining is mainly absent 24 hours after the injection of the patient's serum (C, asterisk) and remained in only the peripheral retina (C, arrows). PKCα staining can be seen 24 hours after the injection of the patient's serum in TRPM1 knockout mouse retina (D arrows). High magnification micrograph showed that the PKC α positive cell bodies were located mainly on the photoreceptor side of the INL. The scale bars are: 60 μm for A left, B left, C upper left and D left; 20 μm for A, B, C and D right; 30 μm for C lower left.

doi: 10.1371/journal.pone.0081507.g004

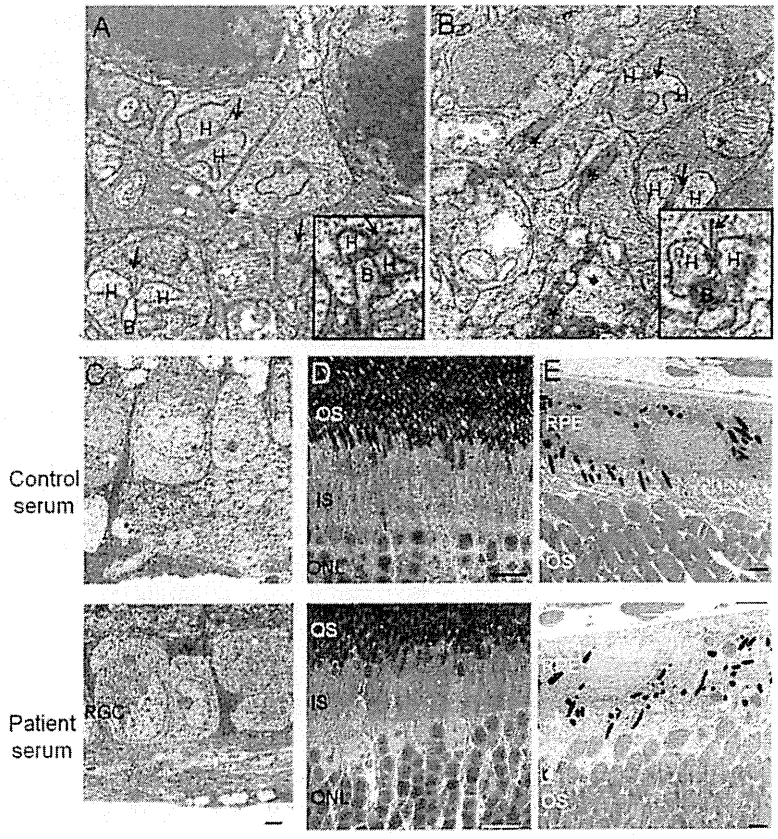

Figure 5. Ultrastructure of other parts of the retina 5 hours after serum injection. (A ,B) Photomicrographs of synaptic terminals between photoreceptors and rod ON bipolar cells are shown. Wild mouse retina injected intravitreally with control serum (A) or with patient's serum (B). The arrows point to the photoreceptor synaptic ribbons. The photoreceptor synaptic ribbons are surrounded by dendrites of two horizontal cells and one invaginating rod ON bipolar cell (4A,insertion). After the injection of the patient's serum, invaginated rod ON bipolar cell dendritic terminals that extended to ribbon synapses were darkly stained (B, asterisk and insertion). (C, D, and E) After the patient's serum injection (lower), the retinal ganglion cells (RGCs), ONL, inner segments of photoreceptors(IS), outer segments of photoreceptors (OS), and retinal pigment epithelium (RPE) showed no abnormalities compared with the retina treated with control serum (upper). The scale bar; A and B = 500 nm; C and E = 2 μm; D = 10 μm. Abbreviations: H - horizontal cell, B - ON bipolar cells.

doi: 10.1371/journal.pone.0081507.g005

400μm , 800μm and 1200 inferior to the optic disc were defined I-3,I-2, and I-1 respectively. The combined INL+OPL in the mice injected with the patient's serum was significantly thinner than that in mice injected control serum at S-2, I-2, and I-1. However, the thickness of the ONL was not significantly different between the two groups at any measured points. To avoid the effects of cutting biases, i.e., not sectioning in the vertical plane, we also checked the ratio of INL+OPL/ONL. The ratios of INL+OPL/ONL were significantly different between the two groups at all sites except I-3. These results supported the conclusion that ON bipolar cells were lost.

We also examined the distribution of ON bipolar cells 3 months after the injection of the serum (Figure 7C). PKCα-positive staining was found over the entire retina 3 months after the control serum injection (Figure 7C upper, arrows). On the other hand, PKCα-positive staining was observed only in the peripheral retina (Figure 7C lower, arrows). These results are similar to those at 24 h after the injection and indicated that the ON bipolar cells degenerated soon after the patient serum injection, and they did not regenerate.

We also examined the OPL by TEM (Figure 7D). The neuropil of the OPL was less dense compared to that of the retina that received control serum (Figure 7D right, asterisk). Some cellular debris was found in the OPL of the patient's serum injected retina (Figure 7D right, arrows).

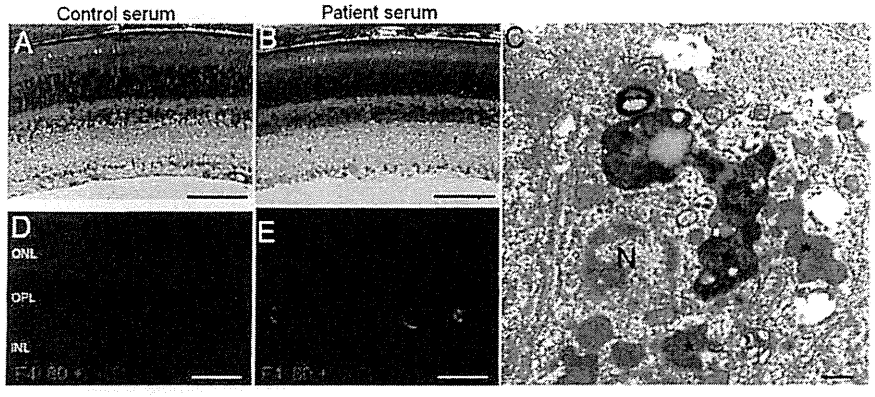

Figure 6. Macrophages are present in the INL 3 days after PR patient's serum was injected. Toluidine blue staining (A and B) and TEM micrographs (C) are of a retina 3 days after the intravitreous injection of the sera. F4/80 immunostaining (green) was co-stained with DAPI (D and E). Wild mouse retina after injection of control serum (A and D) and patient's serum (B, C, and E) are shown. (B) No obvious abnormality can be seen after the patient's serum injection. (C) TEM shows nucleus of macrophage and engulfing the apoptotic cells (N indicates the nucleus of a macrophage, asterisk indicates debris of engulfed apoptotic cells). F4/80 (green) positive cell can be seen in the INL (E). The scale bars; (A) and (B) = 100 μm; (C) = 500 nm; (D) and (E) = 20 μm.

doi: 10.1371/journal.pone.0081507.g006

Discussion

Comparisons with clinical findings in paraneoplastic retinopathy

Our results showed that the intravitreal injection of serum containing an autoantibody against TRPM1 caused ON bipolar cell degeneration within 5 hours. Because the antigen for the autoantibody against ON bipolar cells has not been identified until recently, the mechanism of the ON bipolar cell dysfunction in patients with PR was not known. Two LM histopathological studies of postmortem retinas of MAR patients had conflicting results; one reported no anatomic abnormalities throughout the retina [6] and the other reported a marked reduction in the number of nuclei in the INL [32]. Even if the ON bipolar cells of PR patients degenerate as they did in our mouse model, we believe that it would be difficult to detect the changes by light microscopy because the cellular organization of retina obtained 3 months after the serum injections appeared almost normal by light microscopy (Figure 7A). However, we did find that the thickness of the combined INL+OPL of the mouse retina treated with the patient's serum was thinner than that of control (Figure 7B). Because the difference was slight, it would have been difficult to draw a conclusion from one MAR patient because the thickness of human retina is variable.

Lei and colleagues reported that an intravitreal injection of purified IgG from a MAR patient into monkey eyes led to a reduction in the amplitude of the photopic ERG b-waves [33]. They also reported that the reduction of the b-wave was transient, and the b-wave recovered 3 months after the IgG injection. They also reported injection of the MAR serum into rodent eyes (rat and guinea pig) had no effect on the ERG. We cannot explain the difference from our findings but we suggest that the mechanism for the ON bipolar cell dysfunction is probably different from that of our mice because our results showed a permanent damage. This discrepancy may also be because of the difference in the species examined, concentration of the antibody, relative size of the eye, and injected volume. Another more likely possibility was that the antigen of the IgG was not TRPM1. An antibody against TRPM1 was found in only about 10% of MAR patients in one study [11], and in 2 of 3 MAR patients in another study [10]. These reports indicated that there may be other antigens that can cause MAR in some patients.

There is a report that the signs and symptoms improve in some MAR patients after therapy [6] and other antigens of IgG may have induced the transient ON bipolar dysfunction in these patients. We suggest that an autoantibody against TRPM1 may not apply to all the cases with this syndrome [6].

ERGs of patient and serum-injected mice

The ERGs recorded after APB-injected mice resembled those of mice after the injection of the PR patient's serum; under scotopic and photopic condition, the ERG b-waves were markedly reduced and the amplitude of scotopic a-wave was almost normal. Because it is known that APB blocks ON bipolar cell activity, these results suggested a dysfunction of the ON bipolar cells after the patient's serum injection.

Another retinal disease with ON bipolar cell dysfunction is the complete type of congenital stationary night blindness (cCSNB). The ERGs recorded from patients with cCSNB are similar to those recorded from patients with PR, viz., a marked reduction of the b-wave under scotopic conditions and preserved b-wave under photopic conditions. cCSNB is caused by mutations in the genes that mediate the transduction cascade of the ON bipolar cells, and the symptoms and retinal changes do not change throughout life [34-37]. Mouse models for cCSNB do not have obvious changes in the retinal cellular organization but there is a functional loss of ON bipolar cells.

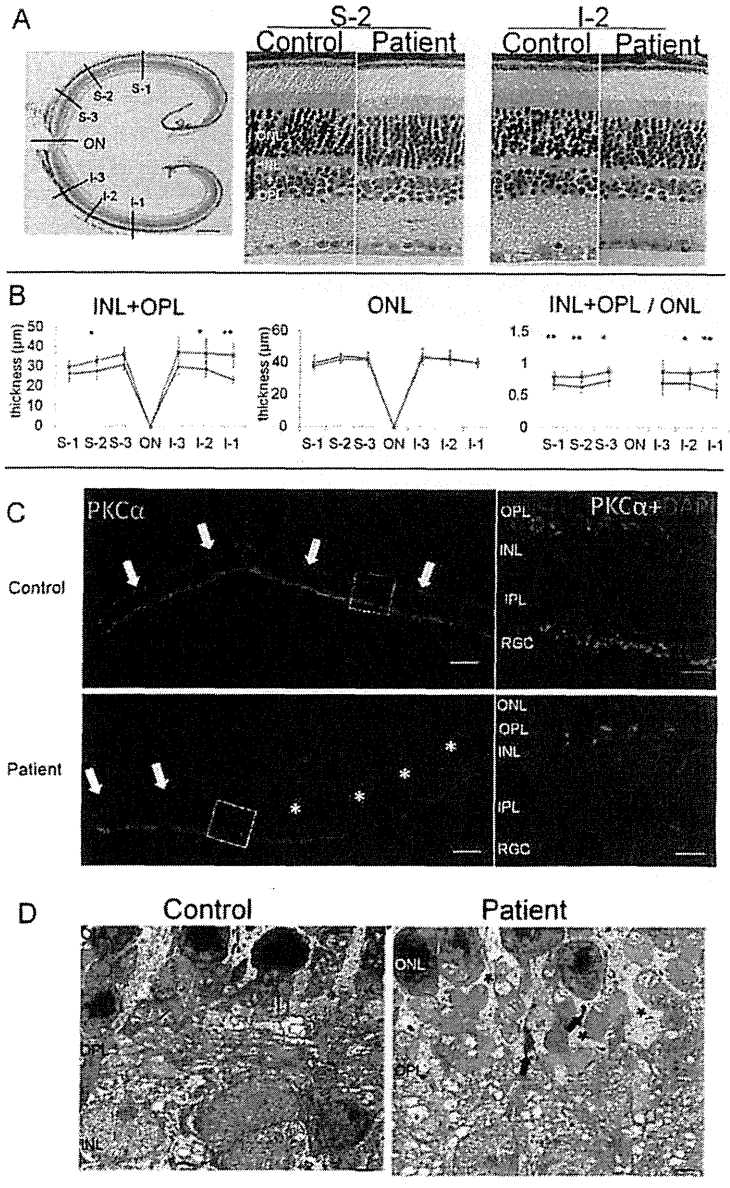

Figure 7. Retina obtained 3 months after the serum injection. (A) HE staining of retina from a mouse that received an intravitreal injection of control or patient's serum 3 months earlier. The thickness of the different layers was measured every 400 μm across both the superior (S1-3) and inferior hemispheres (I1-3) as shown in the low magnification micrograph on the left. Two locations of the retinas are shown (right side of A). The measurement points of the INL+OPL and the ONL are shown by the arrows. The thickness of the INL+OPL, the ONL, and the ratio of INL+OPL/ ONL are shown in (B) (n = 6). The data are the means ± SDs. (*P <0.05 and **P <0.01). .

Distribution of ON bipolar cell marker (PKCα) in the retina 3 months after the injection of serum from a control subject or from the PR patient (C). Photomicrographs of the regions outlined by the white boxes are enlarged to the right. PKCα staining can be seen in the entire retina after the serum from the control subject (C upper, arrows). But PKC staining was mostly absent 3 months after the injection of the patient's serum (C lower, asterisk) and remained only in the peripheral retina (C lower, arrows). (D) Ultrastructure of OPL 3 months after serum injection. The retina of the mouse that received an intravitreal injection of the control serum (left) and the patient's serum (right) are shown. Some of neuropils in the OPL were absent (D right, asterisk) and some debris (D left, arrows) can be seen in the retina after the injection of the patient's serum. The scale bar; A, left = 150 μm; A, right = 20 μm; C, left = 60 μm; C, right = 15 μm; D = 2 μm.

doi: 10.1371/journal.pone.0081507.g007

The waveforms of the mouse ERGs in the eyes that received the patient's serum resembled those of the mouse model of cCSNB [25,38]. Under photopic conditions, there is a difference in the shape of the ERGs between human and mice that have ON bipolar cell dysfunction. This difference was most likely present because the mouse photopic b-waves originate mainly from ON bipolar cells but the human photopic b-waves originate from both the ON and OFF bipolar cells [39]. Thus, the positive OFF response remains even after the loss of the ON bipolar cell response. The shared features of the ERGs between the patients and the mice injected with the patient's serum suggest that the two species also share the pathomechanism of the ON bipolar cell dysfunction. But we have to consider the differences in the immune responses between humans and mice because the mouse retina injected with human IgG and the patient retina affected by human IgG may respond differently.

Apoptotic cells in inner nuclear layer

The most interesting finding of this study was that the serum-containing autoantibody killed the ON bipolar cells very quickly. Our results showed that some of the inner nuclear cells were degenerated as early as 5 hours after the intravitreal injection of the patient's serum (Figure 3), and apoptotic cell death was detected by TUNEL staining at 1 day postinjection. Electon microscopy (Figure 3E and H) showed nuclear condensation which indicated apoptosis of these cells. Because there are many different types of cells in the INL, e.g., ON bipolar cells, OFF bipolar cells, Mueller cells, horizontal cells, and amacrine cells, it was difficult to determine which type was the apoptotic cell. We were not able to show that the TUNEL positive cells were the retinal ON bipolar cells by double labeling with ON bipolar cell maker (PKCα) because the ON bipolar cells had already disappeared (see Figure 4) by 1 day postinjection. In addition, 5 hours was too early to detect TUNEL positive cells. However, we found that the apoptotic cells were located on the photoreceptor side of the INL which is where the ON bipolar cell nuclei are located (Figure 4) [27,40]. In addition, the dendritic tips that invaginated into the photoreceptor synapses were the ones that were darkly stained. Because this is the location of the ON bipolar cell dendritic tips, our findings indicated that the ON bipolar cells were degenerated (Figure 4). Thus, we conclude that the apoptotic cells in the INL were ON bipolar cells, and the negative waveform of the ERGs and extinguished ON bipolar cell marker supported this.

Removal of degenerated ON bipolar cells

Macrophages were found surrounding the apoptotic cells in the INL (Figure 5C). In a mouse model of retinal detachment, the degenerated photoreceptors were removed by macrophages [41]. In our model, the degenerated bipolar cells were probably also removed in the same way. After the clearance of the apoptotic bipolar cells, the retinal architecture appeared to be well organized except for a thinning of the INL +OPL. Because the ERGs did not recover even at 6 months after the injection of the serum and most of the rod ON bipolar cell maker (PKCα) was absent at 3 months after injection, the rod ON bipolar cells most likely did not regenerate. Thus, we conclude that the reduction of the b-wave was due to the loss of ON-bipolar cell, and the change is permanent.

Comparisons of eye manifestations in patients and mice

Patients with PR present with acute night blindness, and our results in mice suggest that the acute apoptosis of the ON bipolar cells may have been the cause of the symptom and signs of PR patients. Optical coherence tomography (OCT) showed that the morphology of the patient's retina was normal [11]. These OCT data indicate that the alterations in the morphology of the patient's retina might be very slight as we showed in the light microscopic images of the retina with almost normal appearances 3 months after the patient serum injection (Figure 7A).

Our PR patient had chemotherapy and now is in complete remission but his symptoms and ERG changes have not recovered. Our morphological data suggest degenerated ON bipolar cells did not regenerate. In patients, fluorescein angiography showed that PR patients have leakage from the retinal blood vessels [11], and it is likely that the autoantibodies leaked out to reach the ON bipolar cells. Thus, we suggest that antibodies directly affected the TRPM1 channels of the ON bipolar cell in both the patient and mice.

The reason we were able to detect ON bipolar cell dysfunction in mice similar to that in PR patients may be because TRPM1 is a membrane protein and the autoantibody easily recognizes the antigen. We believe that our animal model system will be useful for analyzing the mechanism of PR, especially in the cases antigens that are membrane proteins.

Our study has some limitations. We used the serum of just one PR patient, however only six PR patients who have the TRPM1 autoantibody have been reported worldwide. Thus, it would be interesting to investigate the effect of other autoantibodies found in these PR patients.

Conclusions

Our results show that an intravitreal injection of the serum of a patient with PR into the vitreous of mice led to alterations of the ERG that resembled those of the patient with PR. Histological analysis showed that the ON bipolar cells die by apoptosis. As best as we can determine, there has been no previous report of a specific degeneration of retinal ON bipolar cells in hereditary or acquired retinal diseases.

Acknowledgements

We thank Professor Duco Hamasaki of the Bascom Palmer Eye Institute for the discussions and editing the final version of the manuscript. We thank Dr. Takahisa Furukawa for kindly supplying the of antibody, vector and mice. We thank Dr. Jiro Usukura, Dr. Rikako Sanuki, and Dr. Toshio Hisatomi for helpful discussions. We wish to acknowledge Division for Medical Research Engineering, Nagoya University Graduate School of Medicine, for use of their confocal microscope.

Author Contributions

Conceived and designed the experiments: SU KMN AE NK MT. Performed the experiments: SU H. Tanioka AE TY. Analyzed the data: SU TRY SY. Contributed reagents/materials/analysis tools: MK H. Terasaki. Wrote the manuscript: SU KMN.

References

1. Sawyer RA, Selhorst JB, Zimmerman LE, Hoyt WF (1976) Blindness caused by photoreceptor degeneration as a remote effect of cancer. Am J Ophthalmol 81: 606-613. PubMed: 179323.
2. Thirkill CE, Tait RC, Tyler NK, Roth AM, Keltner JL (1992) The cancer-associated retinopathy antigen is a recoverin-like protein. Invest Ophthalmol Vis Sci 33: 2768-2772. PubMed: 1388144.
3. Milam AH, Saari JC, Jacobson SG, Lubinski WP, Feun LG et al. (1993) Autoantibodies against retinal bipolar cells in cutaneous melanoma-associated retinopathy. Invest Ophthalmol Vis Sci 34: 91-100. PubMed: 8425845.
4. Heckenlively JR, Ferreyra HA (2008) Autoimmune retinopathy: A review and summary. Semin Immunopathol 30: 127-134. doi:10.1007/s00281-008-0114-7. PubMed: 18408929.
5. Jacobson DM, Adamus G (2001) Retinal anti-bipolar cell antibodies in a patient with paraneoplastic retinopathy and colon carcinoma. Am J Ophthalmol 131: 806-808. doi:10.1016/S0002-9394(00)00925-9. PubMed: 11384586.
6. Keltner JL, Thirkill CE, Yip PT (2001) Clinical and immunologic characteristics of melanoma-associated retinopathy syndrome: Eleven new cases and a review of 51 previously published cases. J Neuroophthalmol 21: 173-187. doi:10.1097/00041327-200109000-00004. PubMed: 11725182.
7. Berson EL, Lessell S (1988) Para-neoplastic night blindness with malignant-melanoma. Am J Ophthalmol 106: 307-311. doi:10.1016/0002-9394(88)90366-2. PubMed: 2971322.
8. Alexander KR, Fishman GA, Peachey NS, Marchese AL, Tso MOM (1992) On response defect in paraneoplastic night blindness with cutaneous malignant-melanoma. Invest Ophthalmol Vis Sci 33: 477-483. PubMed: 1544774.
9. Goetgebuer G, Kestelyn-Stevens A-M, De Laey J-J, Kestelyn P, Leroy BP (2008) Cancer-associated retinopathy (CAR) with electronegative ERG: a case report. Doc Ophthalmol 116: 49-55. doi:10.1007/s10633-007-9074-9. PubMed: 17721792.
10. Dhingra A, Fina ME, Neinstein A, Ramsey DJ, Xu Y et al. (2011) Autoantibodies in melanoma-associated retinopathy target TRPM1 cation channels of retinal ON bipolar cells. J Neurosci 31: 3962-3967. doi:10.1523/JNEUROSCI.6007-10.2011. PubMed: 21411639.
11. Kondo M, Sanuki R, Ueno S, Nishizawa Y, Hashimoto N et al. (2011) Identification of autoantibodies against TRPM1 in patients with paraneoplastic retinopathy associated with ON bipolar cell dysfunction. PLoS One e19116: e19911
12. Zimov S, Yazulla S (2004) Localization of vanilloid receptor 1 (TRPV1/VR1)-like immunoreactivity in goldfish and zebrafish retinas: restriction to photoreceptor synaptic ribbons. J Neurocytol 33: 441-452. doi:10.1023/B:NEUR.0000046574.72380.e8. PubMed: 15520529.
13. Morgans CW, Zhang J, Jeffrey BG, Nelson SM, Burke NS et al. (2009) TRPM1 is required for the depolarizing light response in retinal ON-bipolar cells. Proc Natl Acad Sci U S A 106: 19174-19178. doi:10.1073/pnas.0908711106. PubMed: 19861548.
14. Koike C, Obara T, Uriu Y, Numata T, Sanuki R et al. (2010) TRPM1 is a component of the retinal ON bipolar cell transduction channel in the mGluR6 cascade. Proc Natl Acad Sci U S A 107: 332-337. doi:10.1073/pnas.0912730107. PubMed: 19966281.
15. Rogers SW, Andrews PI, Gahring LC, Whisenand T, Cauley K et al. (1994) Autoantibodies to glutamate-receptor glur3 in rasmussens encephalitis. Science 265: 648-651. doi:10.1126/science.8036512. PubMed: 8036512.
16. Whitney KD, McNamara JO (2000) GluR3 autoantibodies destroy neural cells in a complement-dependent manner modulated by complement regulatory proteins. J Neurosci 20: 7307-7316. PubMed: 11007888.
17. Dalmau J, Gleichman AJ, Hughes EG, Rossi JE, Peng X et al. (2008) Dessain SK, Rosenfeld MR, Balice-Gordon R, Lynch DR: Anti-NMDA-receptor encephalitis: case series and analysis of the effects of antibodies. Lancet Neurol 7:1091-1098
18. Slaughter MM, Miller RF (1981) 2-amino-4-phosphonobutyric acid: a new pharmacological tool for retina research. Science 211: 182-185.
19. Ueno S, Kondo M, Miyata K, Hirai T, Miyata T et al. (2005) Physiological function of S-cone system is not enhanced in rd7 mice. Exp Eye Res 81: 751-758. doi:10.1016/j.exer.2005.04.013. PubMed: 16005871.
20. Bush RA, Sieving PA (1994) A proximal retinal component in the primate photopic ERG a-wave. Invest Ophthalmol Vis Sci 35: 635-645. PubMed: 8113014.
21. Ueno S, Kondo M, Niwa Y, Terasaki H, Miyake Y (2004) Luminance dependence of neural components that underlies the primate photopic electroretinogram. Invest Ophthalmol Vis Sci 45: 1033-1040. doi:10.1167/iovs.03-0657. PubMed: 14985327.
22. Brown KT (1969) The electroretinogram: its components and their origins. UCLA Forum Med Sci 8: 319-378. PubMed: 4990860.
23. Granit R (1933) The components of the retinal action potential in mammals and their relation to the discharge in the optic nerve Part I Isolation of components in the retinal action potential of the dark-adapted decerebrate preparation. J Physiol-London 77: 207-239. PubMed: 16994385.
24. Machida S, Kondo M, Jamison JA, Khan NW, Kononen LT et al. (2000) P23H rhodopsin transgenic rat: Correlation of retinal function with histopathology. Invest Ophthalmol Vis Sci 41: 3200-3209. PubMed: 10967084.
25. Masu M, Iwakabe H, Tagawa Y, Miyoshi T, Yamashita M et al. (1995) Specific deficit of the on response in visual transmission by targeted disruption of the mGluR6 gene. Cell 80: 757-765. doi:10.1016/0092-8674(95)90354-2. PubMed: 7889569.
26. Grünert U, Martin PR, Wässle H (1994) Immunocytochemical analysis of bipolar cells in the macaque monkey retina. J Comp Neurol 348: 607-627. doi:10.1002/cne.903480410. PubMed: 7530731.
27. Ruether K, Feigenspan A, Pirngruber J, Leitges M, Baehr W et al. (2010) PKC alpha Is Essential for the Proper Activation and Termination of Rod Bipolar Cell. Response - Invest Ophthalmol Vis Sci 51: 6051-6058. doi:10.1167/iovs.09-4704.
28. Kolb H, Zhang L, Dekorver L (1993) Differential staining of neurons in the human retina with antibodies to protein kinase C isozymes. Vis Neurosci 10: 341-351. doi:10.1017/S0952523800003734. PubMed: 8485096.
29. Vardi N (1998) Alpha subunit of G(0) localizes in the dendritic tips of ON bipolar cells. J Comp Neurol 395: 43-52. doi:10.1002/(SICI)1096-9861(19980525)395:1. PubMed: 9590545.
30. Ichikawa M, Arissian K, Asanuma H (1985) Distribution of corticocortical and thalamocortical synapses on identified motor cortical neurons in the cat: Golgi, electron microscopic and degeneration study. Brain Res 345: 87-101. doi:10.1016/0006-8993(85)90839-X. PubMed: 2998551.
31. Leong SK, Wong WC (1989) An ultrastructural study of the stellate ganglion of the pig-tailed monkey (Macaca nemestrina). J Anat 164: 1-18. PubMed: 2606786.
32. Gittinger JW Jr., Smith TW (1999) Cutaneous melanoma-associated paraneoplastic retinopathy: histopathologic observations. Am J Ophthalmol 127: 612-614. doi:10.1016/S0002-9394(98)00431-0. PubMed: 10334362.
33. Lei B, Bush RA, Milam AH, Sieving PA (2000) Human melanoma-associated retinopathy (MAR) antibodies alter the retinal ON-response of the monkey ERG in vivo. Invest Ophthalmol Vis Sci 41: 262-266. PubMed: 10634629.
34. Miyake Y, Yagasaki K, Horiguchi M, Kawase Y, Kanda T (1986) Congenital stationary night blindness with negative electroretinogram - A new classification. Arch Ophthalmol 104: 1013-1020. doi:10.1001/archopht.1986.01050190071042. PubMed: 3488053.
35. Bech-Hansen NT, Naylor MJ, Maybaum TA, Sparkes RL, Koop B et al. (2000) Mutations in NYX, encoding the leucine-rich proteoglycan nyctalopin, cause X-linked complete congenital stationary night blindness. Nat Genet 26: 319-323. doi:10.1038/81619. PubMed: 11062471.
36. Dryja TP, McGee TL, Berson EL, Fishman GA, Sandberg MA et al. (2005) Night blindness and abnormal cone electroretinogram ON responses in patients with mutations in the GRM6 gene encoding mGluR6. Proc Natl Acad Sci U S A 102: 4884-4889. doi:10.1073/pnas.0501233102. PubMed: 15781871.
37. Pusch CM, Zeitz C, Brandau O, Pesch K, Achatz H et al. (2000) The complete form of X-linked congenital stationary night blindness is

caused by mutations in a gene encoding a leucine-rich repeat protein. Nat Genet 26: 324-327. doi:10.1038/81627. PubMed: 11062472.
38. Pardue MT, McCall MA, LaVail MM, Gregg RG, Peachey NS (1998) A naturally occurring mouse model of X-linked congenital stationary night blindness. Invest Ophthalmol Vis Sci 39: 2443-2449. PubMed: 9804152.
39. Sieving PA, Murayama K, Naarendorp F (1994) Push-pull model of the primate photopic electroretinogram - A role for hyperpolarizing neurons in shaping the b-wave. Vis Neurosci 11: 519-532. doi:10.1017/S0952523800002431. PubMed: 8038126.
40. Jeon CJ, Strettoi E, Masland RH (1998) The major cell populations of the mouse retina. J Neurosci 18: 8936-8946. PubMed: 9786999.
41. Hisatomi T, Sakamoto T, Sonoda KH, Tsutsumi C, Qiao H et al. (2003) Clearance of apoptotic photoreceptors - Elimination of apoptotic debris into the subretinal space and macrophage-mediated phagocytosis via phosphatidylserine receptor and integrin alpha v beta 3. Am J Pathology 162: 1869-1879. doi:10.1016/S0002-9440(10)64321-0.

Relationship Between Retinal Layer Thickness and Focal Macular Electroretinogram Components After Epiretinal Membrane Surgery

Nobuaki Hibi,[1] Shinji Ueno,[1] Yasuki Ito,[1] Chang-Hua Piao,[1] Mineo Kondo,[1,2] and Hiroko Terasaki[1]

[1]Department of Ophthalmology, Nagoya University Graduate School of Medicine, Nagoya, Japan
[2]Department of Ophthalmology, Mie University Graduate School of Medicine, Tsu, Japan

Correspondence: Shinji Ueno, Department of Ophthalmology, Nagoya University Graduate School of Medicine, 65 Tsuruma-cho, Showa-ku, Nagoya 466-8550, Japan; ueno@med.nagoya-u.ac.jp.

Submitted: July 22, 2013
Accepted: September 22, 2013

Citation: Hibi N, Ueno S, Ito Y, Piao C-H, Kondo M, Terasaki H. Relationship between retinal layer thickness and focal macular electroretinogram components after epiretinal membrane surgery. *Invest Ophthalmol Vis Sci.* 2013;54:7207–7214. DOI: 10.1167/iovs.13-12884

Purpose. To study the effect of epiretinal membrane (ERM) removal on the function and structure of the retina, and to determine whether the functional changes were correlated with the changes in the thickness of different retinal layers.

Methods. Focal macular electroretinography (FMERG) and spectral-domain optical coherence tomography (SD-OCT) were performed on 17 eyes of 15 patients before and after ERM surgery. The parafoveal retina was divided into an inner layer, a middle layer, and an outer layer in the OCT images. The thickness of each layer was measured before and after the ERM surgery. The a-wave, b-wave, and oscillatory potentials (OPs) of the FMERGs were analyzed before and after the ERM surgery.

Results. The thickness of the inner and middle retinal layers was significantly reduced after surgery (by 39% and 23%, respectively). The mean amplitudes of the b-waves and OPs at 6 months postoperatively were significantly larger than those recorded preoperatively (by 21% and 61%, respectively). The ratios of the pre- to postoperative b-wave and OP amplitudes were correlated with the thickness reduction of the middle retinal layer (b-wave, $r = -0.51$, $P < 0.05$; OPs, $r = -0.82$, $P < 0.01$).

Conclusions. The significant correlations between the reduction in the thickness of the middle retinal layer and increase in the amplitude of the b-waves and OPs suggest that the improvement of macular function after ERM peeling is due to the decrease in the thickness of the middle retinal layer.

Keywords: idiopathic epiretinal membrane, optical coherence tomography, focal macular electroretinograms

An idiopathic epiretinal membrane (ERM) is a relatively common macular disease in aging patients.[1] An ERM on the macula causes traction on the retina, leading to a distortion of vision and/or a decrease of visual acuity. The surgical treatments for an ERM include vitrectomy with ERM peeling, and successful removal results in improved visual function.

To study an ERM or examine the effects of ERM removal on the retina, clinicians have used optical coherence tomography (OCT), which can obtain cross-sectional images of the retina with micrometer resolution and good repeatability. Optical coherence tomography is performed noninvasively and quantitative measurements of the different layers of the retina can be made. Earlier OCT studies have shown the morphologic features of an ERM.[2–12] The results of these studies have shown that the visual dysfunction in eyes with an ERM is due to a thickening of the macular area, and a reduction in the thickness after surgery is accompanied by improvements of macular function.[2,3,5,6,9] Most of the earlier studies use subjective tests, such as visual acuity,[3,5–8] Amsler grid,[12] and M-CHARTS,[11] to assess the retinal function of ERM patients. Other studies use objective methods including multifocal electroretinograms[13–15] and focal macular electroretinograms (FMERGs).[16–19]

Because our laboratory believed that examination of the different components of the FMERGs was an informative way to evaluate the pathophysiology and function of the macular area, we have used FMERGs to analyze the functions of many retinal diseases.[16,17,19–25] We have found that the degree of reduction of the oscillatory potentials (OPs) of the FMERGs is relatively greater than the reduction of the a- and b-waves in eyes with an ERM.[16,17,19] If the sensory retina is divided into "inner" and "outer" layers, we have suggested that an ERM impairs the function predominantly of the inner retinal layer.[16,17,19]

However, the OCT instruments at the time of those studies did not have enough spatial resolution to detect finer changes in the retinal structure. Recent advancements of OCT technology, for example, spectral-domain OCTs (SD-OCTs), have made it possible to view and measure the retinal structures more accurately with better resolution. This has allowed clinicians to measure the thicknesses of the different retinal layers.[8–12,26,27]

The results of these earlier studies indicate that the visual acuity in eyes with an ERM is significantly associated with the thickness of the inner nuclear layer (INL).[9,12] However, other studies report that the visual acuity is associated with alterations of the outer retinal layer or the photoreceptors.[8,27]

www.iovs.org | ISSN: 1552-5783

Investigative Ophthalmology & Visual Science

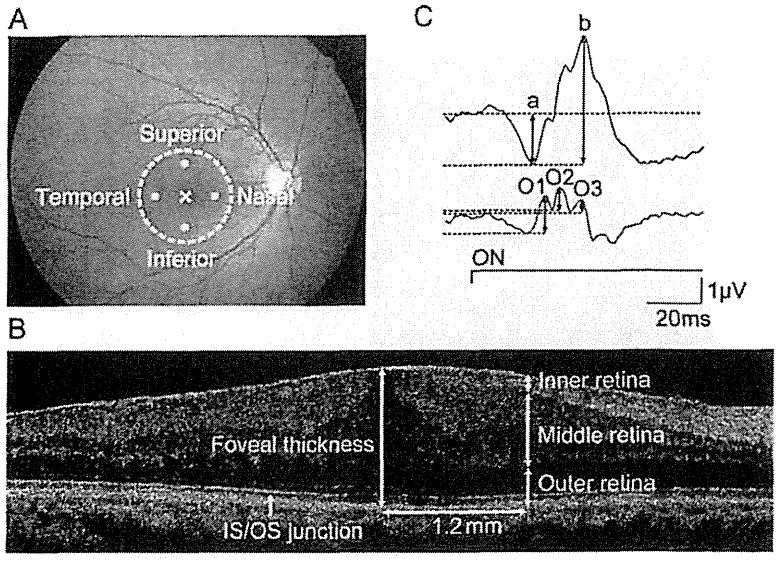

FIGURE 1. Measurements of retinal layers in the SD-OCT images and components of FMERGs. (A) Fundus of a normal right eye. *Four white dots* are placed 1.2 mm from the foveal pit. The parafoveal layer thicknesses at these 4 points were measured in the SD-OCT images. The *white circle* indicates the stimulus spot of 15° used to elicit the FMERGs. (B) SD-OCT image of a 6-mm horizontal scan. Parafoveal retina was segmented into the inner, middle, and outer retina in the OCT image. The inner retina includes the ERM and RNFL. The middle retina includes the retinal GCL, IPL, INL, and OPL. The outer retina includes the photoreceptor layer and RPE. The IS/OS junction is indicated by an *arrow*. (C) FMERGs recorded from a normal eye. A bandpass filter limiting the responses to those between 5 to 500 Hz was used to record the a- and b-wave (*upper*), and a bandpass filter from 50 to 500 Hz was used to extract the OPs (*lower*). The sum of O1, O2, and O3 amplitudes was used for the statistical analyses.

In addition, others have demonstrated that the visual function is associated with both the INL and photoreceptor misalignment.[10,11] One difficulty in interpreting the results of these earlier studies is the fact that the ERM surgeries are performed simultaneously with cataract surgery, and it is not possible to eliminate the additional effects of a clearer optical pathway. Thus, FMERGs became a valuable method to assess the retina after any type of treatment. Because the a- and b-waves, OPs, and other components of the FMERGs originate from different retinal layers, they can be used not only to analyze the macular function objectively but also to evaluate the function of the retina layer by layer.

Thus, the purpose of this study was to determine the relationship between the thickness of the different retinal layers and macular function after ERM surgery. To accomplish this, we recorded FMERGs before, and 3 and 6 months after, surgery and measured the thickness of the different retinal layers in the SD-OCT images recorded at the same times.

PATIENTS AND METHODS

Fifteen consecutive patients who underwent surgery to remove an idiopathic ERM at Nagoya University Hospital between October 2010 and July 2012 by a single surgeon (HT) were recruited for this study. Patients with a secondary ERM, significant cataracts, glaucoma, and excessive myopia (more than −6.0 diopters or an axial length > 25 mm) were excluded. Seventeen eyes of the 15 patients (7 men and 8 women) who agreed to participate in this study and were willing to be followed up for at least 6 months after the surgery were enrolled. The mean age ± standard deviation was 68.9 ± 7.6 years with a range from 59 to 88 years.

Standard 3-port pars plana vitrectomy was performed on 6 eyes with a 23-gauge system and on 11 eyes with a 25-gauge system. After core vitrectomy, the ERM and internal limiting membrane were peeled with assistance of triamcinolone acetonide. In all cases, the membrane-peeling procedure was performed without the use of indocyanine green. Phacoemulsification with aspiration and intraocular lens implantation were performed during the vitrectomy in all of the eyes.

All of the patients signed an informed consent for the surgery and agreed to the recording of the visual acuity, OCT, and FMERGs during the follow-up examinations. The procedures used in this study were approved by the Institutional Review Board Committee of Nagoya University Graduate School of Medicine (approval No. 2013-0009). All of the procedures conformed to the tenets of the Declaration of Helsinki. A written informed consent was obtained from all the patients after they were provided with information on the procedures to be used.

Best-Corrected Visual Acuity (BCVA)

The best-corrected visual acuity was measured before, and 3 and 6 months after, the surgery. A standard Japanese visual acuity chart was used, and the decimal BCVA was converted to the logarithm of the minimum angle of resolution (logMAR) for the statistical analyses.

Macular Thickness

The macular thickness was measured on the SD-OCT (Cirrus HD-OCT; Carl Zeiss Meditec, Dublin, CA) images before, and 3 and 6 months after, the surgery. The methods we used for the SD-OCT examinations have been described in detail.[28] Five-line vertical and horizontal raster scans of 6-mm length were made, and the scan through the fovea was used to measure the macular thickness. We measured the foveal thickness and parafoveal thicknesses. The parafoveal thickness was calculated as the mean thickness at 1.2 mm nasal, temporal, superior, and inferior to the fovea (Fig. 1A). We selected these points because the foveal pit and the immediate surrounding area lacked the inner retinal layers, which made it not suitable to analyze the different

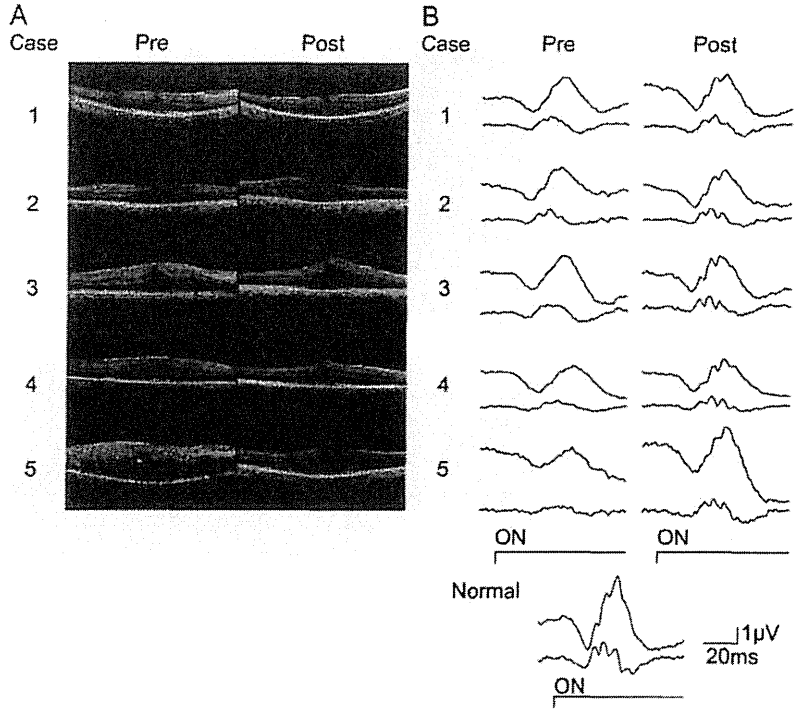

FIGURE 2. Examples of the changes of the OCT images (A) and FMERGs (B) in 5 representative patients before and 6 months after the surgery. The preoperative and 6 months' postoperative images are shown on the *left* and *right*, respectively. (A) Examples of the OCT images of 5 patients. The total and middle macular thickness decreased after surgery in all cases, although the degree of reduction varied. Cases 3 and 5 show a marked decrease of retinal thickness but others show a mild reduction. (B) FMERGs recorded from 5 patients are shown. The extracted OPs of each FMERGs are shown in the *lower trace* beneath the original wave. In all cases, the b-waves and OPs increased after surgery; however, the increase for OPs was greater than that for the b-wave.

retinal cellular layers. Segmentation of the retinal layers was done manually by one experienced masked operator. We divided the retinal layers of parafovea into 3 layers: (1) inner retinal layer consisting of the ERM, inner limiting membrane, and retinal nerve fiber layer (RNFL); (2) a middle retinal layer consisting of the ganglion cell layer (GCL), inner plexiform layer (IPL), inner nuclear layer (INL), and outer plexiform layer (OPL); and (3) an outer retinal layer consisting of the photoreceptor layer and retinal pigment epithelium (RPE). The total retinal thickness was defined as the distance from the vitreoretinal interface to the outer border of the RPE layer.

Integrity of Photoreceptor Inner Segment/Outer Segment Junction Line

The inner segment/outer segment (IS/OS) junction line is a hyperreflexive line in the photoreceptor layer of SD-OCT images as shown in Figure 1B. We assessed the integrity of the IS/OS line in the OCT images preoperatively in all of the patients. We examined the horizontal and vertical images through the fovea. When the IS/OS line in both images was detected to be continuous, we classified the IS/OS line to be "intact," otherwise we classified it to be "disrupted." We analyzed the relationship between preoperative IS/OS line status and the FMERG components.

Focal Macular Electroretinograms

Focal macular electroretinograms (ER-80; Kowa, Nagoya, Japan) were recorded before, and 3 and 6 months after, the surgery. The technique of recording FMERGs under direct fundus observation has been described in detail.[29,30] Briefly, after the patients' pupils were fully dilated with 0.5% tropicamide and 0.5% phenylephrine hydrochloride, a Burian-Allen bipolar contact lens electrode (Hansen Ophthalmic Development Laboratories, Iowa City, IA) was used to record the FMERGs. The size of the stimulus spot was 15° (Fig. 1A), and the background light from the fundus camera (CF-60DSi; Canon, Tokyo, Japan) illuminated nearly the entire visual field. The luminance of the stimulus was 30 cd/m^2, and the background luminance was 1.5 cd/m^2. The position of the spot on the fundus was monitored during the recording with a modified infrared fundus camera (ER-80; Kowa). The responses were digitally bandpass filtered from 5 to 500 Hz for the a- and b-waves and from 50 to 500 Hz for the OPs. Five hundred responses were averaged at a stimulation rate of 5 Hz (Neuropack S1 MEB-9400; Nihon Kohden, Tokyo, Japan). The amplitudes of the a-waves, b-waves, and OPs and the implicit times of a-waves and b-waves of the FMERGs were analyzed. The a-wave amplitude was measured from the baseline to the first negative trough, and the amplitude of the b-wave was measured from the trough of the a-wave to the positive peak of the b-wave (Fig. 1C). Similarly, the implicit time of the a-waves and b-waves was analyzed at the time of the trough of the a-wave and peak of the b-wave. For the OP amplitudes, we measured the amplitude of each OP from the trough to the peak (O1~O3), and the sum of the O1, O2, and O3 amplitudes was used for the statistical analyses (Fig. 1C).[31]

Statistical Analyses

Statistical analyses were performed by using the Spearman rank correlation tests, Wilcoxon signed rank tests, and Student's *t*-

TABLE 1. Results of Visual Acuity, OCT, and FMERG

	Preoperative	Postoperative 3 Months	Postoperative 6 Months
Visual acuity, mean ± SE, logMAR (Snellen)	0.41 ± 0.05 (20/51)	0.13 ± 0.03* (20/27)	0.10 ± 0.03* (20/25)
Foveal thickness, mean ± SE, μm	486.6 ± 28.7	445.4 ± 24.1	424.8 ± 21.2†
Parafoveal thickness, mean ± SE, μm			
Total retina	435.0 ± 15.9	370.9 ± 7.5*	364.8 ± 6.7*
Inner retina	57.1 ± 4.4	37.7 ± 2.4*	35.1 ± 2.2*
Middle retina	222.0 ± 9.9	176.0 ± 4.7*	171.2 ± 4.8*
Outer retina	155.9 ± 4.6	157.2 ± 3.5	158.5 ± 3.6
Amplitude, mean ± SE, μV			
a-Wave	1.04 ± 0.08	1.02 ± 0.10	1.17 ± 0.12
b-Wave	1.98 ± 0.18	2.02 ± 0.17	2.39 ± 0.24†
OPs	0.82 ± 0.08	1.12 ± 0.11†	1.32 ± 0.14*
Implicit time, mean ± SE, ms			
a-Wave	26.5 ± 0.5	25.6 ± 0.3†	25.5 ± 0.3
b-Wave	48.1 ± 0.9	45.7 ± 0.6†	45.8 ± 0.4†

* $P < 0.01$, significance between pre- and postoperative (Wilcoxon signed rank test).
† $P < 0.05$.

tests. The data were analyzed with Statcel software (2nd edition), which is an add-in module for Microsoft Excel (Statcel; OMS, Tokyo, Japan). A $P < 0.05$ was considered to be statistically significant.

RESULTS

Visual Acuity

The mean preoperative BCVA was 0.41 ± 0.05 logMAR units (mean ± SE). The BCVA was 0.13 ± 0.03 logMAR units at 3 months and 0.10 ± 0.03 logMAR units at 6 months. A visual acuity of 0.0 logMAR units corresponds to 20/20 vision on the Snellen chart, and smaller logMAR units indicate better visual acuity. The improvement in the BCVA was significant at both times ($P < 0.001$, Wilcoxon signed rank test).

Macular Thickness

The horizontal OCT images of 5 representative patients obtained preoperatively and at 6 months postoperatively are shown in Figure 2A. The thickness of the macula decreased in all cases but the degree of reduction varied widely. Examination of the pre- and postoperative SD-OCT images showed that the structures of the outer retina were mainly preserved, but the shape of the inner and middle retinal layers were distorted even after the surgery.

The mean foveal thickness was decreased significantly 6 months after the surgery ($P < 0.05$, Wilcoxon signed rank test; Table 1). The mean parafoveal thickness of each retinal layer of the preoperative eyes, the normal fellow eyes, and eyes at 3 and 6 months postoperatively are presented in Figure 3. All retinal layers in the preoperative eyes were significantly thicker

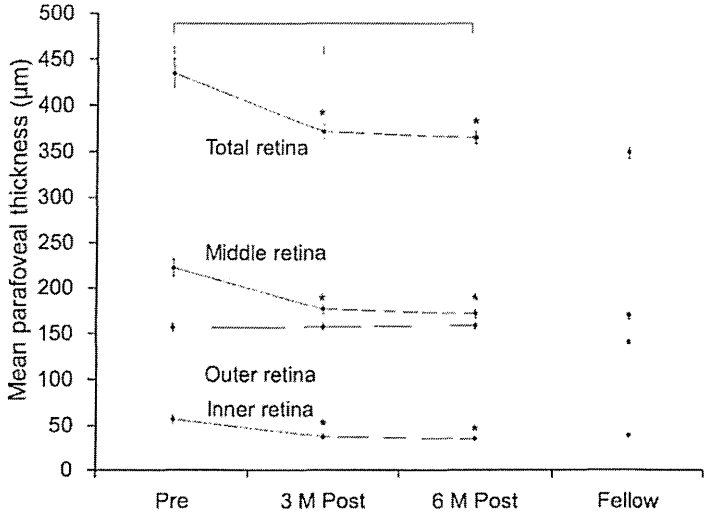

FIGURE 3. The thicknesses of the total, inner, middle, and outer retina before and after surgery are shown. In addition, the retinal thickness of the normal fellow eyes, excluding 2 cases with both eyes affected, is shown. The thickness of the different retinal layers, except the outer retinal layer, is reduced significantly at 3 and 6 months after surgery. *$P < 0.01$ versus baseline (Wilcoxon signed rank test). *Error bars* indicates the SEMs.

Investigative Ophthalmology & Visual Science

TABLE 2. Results of Visual Acuity and FMERG in Preoperative Setting According to IS/OS Status

	IS/OS Status		
	Intact, $n = 7$	Disrupted, $n = 10$	P
Visual acuity, mean ± SE, logMAR (Snellen)	0.3 ± 0.1 (20/44)	0.5 ± 0.1 (20/58)	0.252
Amplitude, mean ± SE, μV			
a-Wave	1.2 ± 0.1	0.9 ± 0.10	0.126
b-Wave	2.6 ± 0.2	1.5 ± 0.2	0.001
OPs	1.1 ± 0.1	0.7 ± 0.1	0.010
Implicit time, mean ± SE, ms			
a-Wave	25 ± 0.5	27 ± 0.7	0.049
b-Wave	46 ± 0.9	50 ± 1.1	0.010

Student's t-test.

than the corresponding layers of the normal fellow eyes ($P < 0.05$, Student's t-test).

After the surgery, the total, inner, and middle retinal layers were significantly thinner at 3 and 6 months than the preoperative thicknesses (Fig. 3 and Table 1; $P < 0.01$, Wilcoxon signed rank test). The reduction occurred mainly during the first 3 months. The thickness of the outer retinal layer did not change until 6 months after the surgery (Fig. 3 and Table 1). There were no significant differences among the thicknesses between the 2 postoperative times.

Focal Macular Electroretinograms

Representative FMERGs from 5 patients recorded before surgery and 6 months postoperatively are shown in Figure 2B. In all cases, the amplitude of the b-waves and OPs increased after surgery, especially in case 5. However, in most cases the FMERGs did not recover to the normal range. The mean amplitudes of the a-waves, b-waves, and sum of OPs and the mean implicit times of the a-waves and b-waves, recorded before surgery and 3 and 6 months postoperatively, are shown in Table 1. The implicit time of b-waves was significantly shorter at 3 and 6 months after the surgery (Wilcoxon singed rank test). The amplitudes of the b-waves and OPs increased significantly at 6 months after surgery (Wilcoxon signed rank test) but that of the a-waves did not change significantly. The mean amplitude of the OPs at 6 months postoperatively was 1.6 times larger than the preoperative amplitude, and the mean amplitude of the b-wave was 1.2 times larger than that of the preoperative b-wave.

Integrity of Photoreceptor IS/OS Junction Line

From the preoperative SD-OCT images, we classified 7 eyes (41%) as having an intact IS/OS line, while 10 eyes (59%) had disrupted IS/OS lines. There were no significant differences in visual acuity and amplitude of the a-wave between the 2 groups (Student's t-test, Table 2). However, there were significant differences in the amplitudes of the b-wave and OPs and the implicit times of the a- and b-waves between the 2 groups (Student's t-test, Table 2).

Correlation Between Retinal Layer Thickness and FMERG Components After ERM Surgery

We determined whether the change of each retinal layer thickness was significantly associated with the improvement of the BCVA and with each component of the FMERGs. We determined the correlation between preoperative and 6 months' postoperative values. An improvement of the BCVA was not correlated with the ratios of the 6 months' postoperative to the preoperative thicknesses at the parafovea for all retinal layers (Supplementary Fig. S1). The 6 M-post/preoperative ratios of the b-wave amplitude were correlated with the post/preoperative ratios of the parafoveal thickness of the total retina ($r = -0.55$, $P = 0.028$, Spearman rank correlation test) and that of the middle retina ($r = -0.51$, $P = 0.042$; Fig. 4). The 6 M-post/preoperative ratios of the sum of the OPs amplitude were also significantly correlated with the post/preoperative ratios of the total retinal thickness ($r = -0.74$,

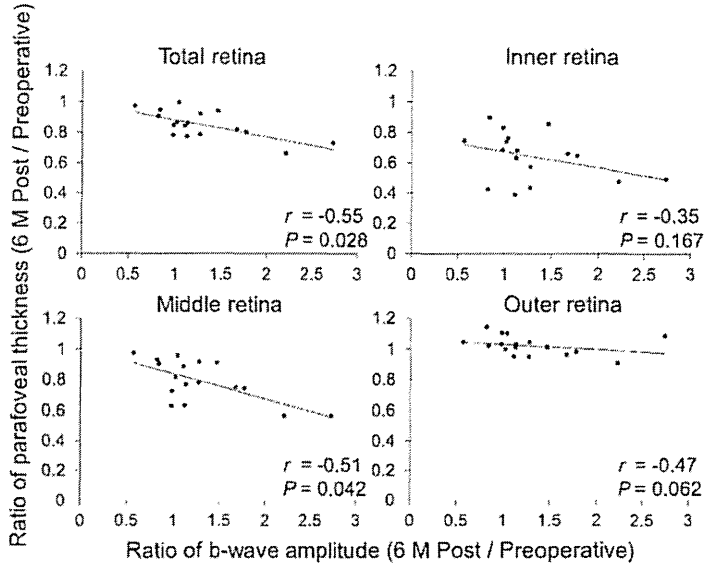

FIGURE 4. Correlations between pre- and postoperative ratios of the b-wave amplitudes at 6 months and the pre- and postoperative ratios of the macular thickness at 6 months. The ratios of the b-wave amplitudes are significantly correlated with the ratios of total and middle retinal thickness (Spearman rank correlation test).

Investigative Ophthalmology & Visual Science

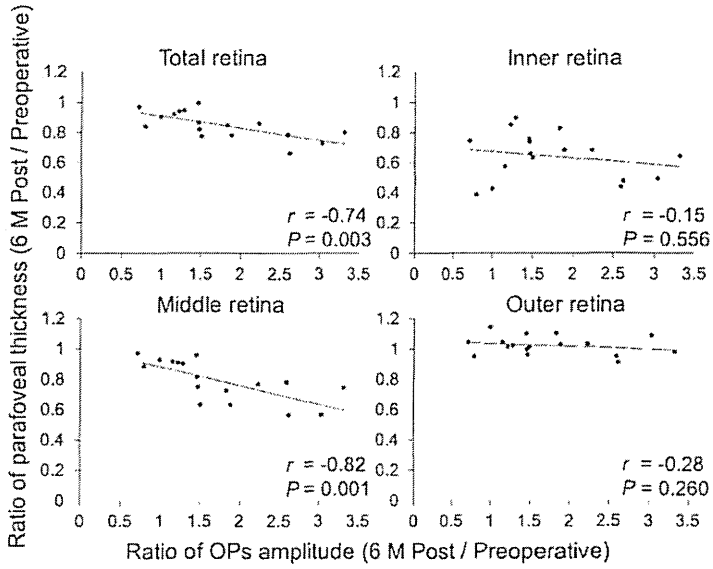

FIGURE 5. Correlations between the pre- and postoperative ratios of the OP amplitude and the pre- and postoperative ratios of the macular thickness at 6 months. The ratios of the OP amplitudes are significantly correlated with the pre- and postoperative ratios of the total and middle retinal thickness (Spearman rank correlation test).

$P = 0.003$) and that of the middle retina ($r = -0.82$, $P = 0.001$; Fig. 5). The coefficient of correlation was higher for the OPs than for the b-waves. In addition, the change of the b-wave implicit time was significantly correlated with the post/preoperative ratios of the middle retinal thickness ($r = 0.50$, $P = 0.046$; Fig. 6).

DISCUSSION

Our SD-OCT results showed that the parafoveal thickness of the inner and middle retinal layers was significantly decreased but the outer retina did not change significantly after the ERM surgery. The mean amplitudes of the FMERG b-waves and OPs were significantly larger postoperatively than those recorded preoperatively. We then determined whether the changes in the thickness of each retinal layer were significantly correlated with the increase in the amplitudes and implicit times of the FMERG. Our analysis showed that the change of thickness in the middle layer, but not inner and outer layer, was significantly correlated with the increase of b-wave and OP amplitude and shortening of b-wave implicit time after ERM peeling. Thus, we confirmed that the improvement of FMERGs by ERM peeling was associated mainly with a reduction of the thickness of the middle retinal layer. Because the coefficient of correlation was

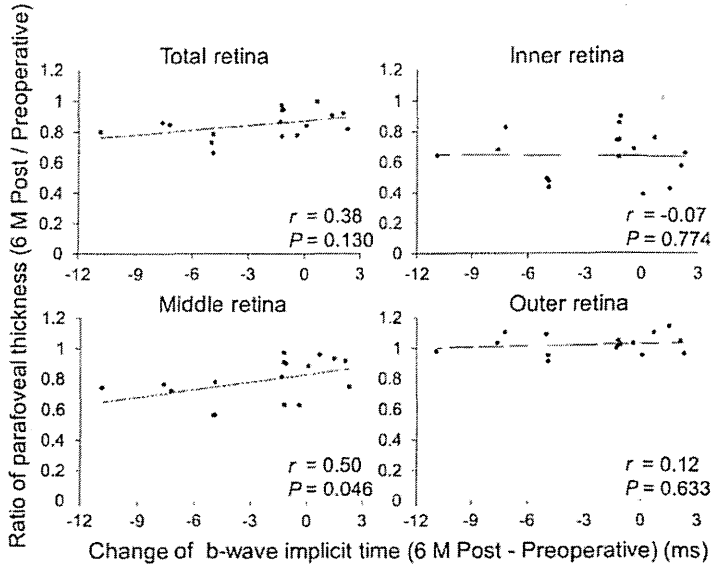

FIGURE 6. Correlations between difference of the b-wave implicit times at 6 months and the pre/postoperative ratios of the macular thickness at 6 months. The difference of the b-wave amplitudes is significantly correlated with the ratios of middle retinal thickness (Spearman rank correlation test).

higher for the relative amplitudes of the OPs than for the b-waves, improvements in the amplitude of the OPs were more strongly correlated with the change in the middle retinal layer thickness than were those of b-waves.

We have reported that the reduction in the amplitude of OPs was significantly greater than that of a-waves and b-waves of the FMERGs of patients with ERM. From these results, we suggest that the ERM probably induces damage mainly to the inner retinal neurons, including the retina from the INL to GCL, because these FMERG components are similarly changed in eyes with cystoid macular edema, which is known to damage the inner retina.[16] We have reported in another study that the reduction of the OPs of the FMERGs does not recover to the normal range after ERM surgery.[17] We assumed that the functional alterations in eyes with an ERM occurs mainly from greater impairment of the inner retina than the outer retina. However, in these studies, we have not been able to confirm the relationship between the thicknesses of the different retinal layers and the FMERG components because of the lower resolution of the OCT instruments at that time. The advancements of OCT technology have enabled us to confirm our earlier assumptions in this study.

A study of the origins of FMERG components, using pharmacologic techniques in monkey retinas, has shown that the b-waves of the FMERGs originate mainly from the ON bipolar cells with additional contribution from the OFF bipolar cell pathway.[32] On the other hand, the origin of the OPs seems to be more from the inner retina than the ON bipolar cells. The results of several full-field ERG studies have suggested that the retinal amacrine cells are the origin of OPs.[33–35] The cell bodies of the ON bipolar cells and amacrine cells are both located in INL, with those of the ON bipolar cells located more in the outer section of the INL and those of the amacrine cells located in the inner section of the INL.[36] We assumed that this difference of location would affect their susceptibility to ERM damage.

One of the commonly used methods to assess macular function is visual acuity. Several studies have examined the relationship between the retinal cell layers and the BCVA in eyes with an ERM.[8,9,12] Kim et al.[9] report that the preoperative parafoveal thicknesses of the GCL+IPL and INL are significantly associated with the preoperative BCVA. Other studies have shown that the degree of metamorphopsia is associated with the macular thickness of the INL.[10–12] These results suggest a similar pathophysiology in eyes with an ERM, indicating that an ERM affects the inner retina more than the outer retina. However, our results showed that the improvement of the BCVA postoperatively was not significantly correlated with the changes in the parafoveal thickness of any of the retinal layers. Even though the BCVA is a relatively easy way to assess the physiology of the fovea, it can be affected by other conditions, such as astigmatism, corneal haze, and cataracts. Because all of our patients underwent cataract surgery, the improvements in the BCVA may have been partially caused by the cataract surgery. This would then mask the relationship with the retinal structure. In addition, the number of patients may have been too low to detect a significant correlation between the thicknesses of the retinal layers and the BCVA.

Other studies have shown that the visual function is significantly associated with the alignment of the photoreceptors.[8,27] Our results also showed that the macular function of eyes that had disrupted IS/OS lines was impaired compared to that of eyes that had intact IS/OS lines. Because the ERMs are located on the surface of the retina, the ERM may disturb the inner retina predominantly in the early stages but the damage may progress to the outer retina in advanced stages.

Our results showed that the amplitudes of the FMERG components were not significantly correlated with the inner retinal thickness. However, this does not mean that the function of the retinal ganglion cells was preserved in eyes with an ERM because the FMERG components analyzed do not originate from the retinal ganglion cell activity.

There were 2 limitations in this study. The first limitation was that we could not measure the macular thickness by macular thickness map owing to the limitation of software. A macular thickness map may allow us to analyze the retinal cell layer 3-dimensionally and to evaluate the retinal structure more precisely. The second limitation was that we did not obtain microperimetry data. It might have helped us to get more information about the sensitivity of each point of retina analyzed by OCT.

In conclusion, the significant correlations between the thickness of the middle retinal layer and the amplitude of the b-waves and OPs suggest that the improvement of macular function after ERM peeling is mainly due to the decrease in the thickness of the middle retinal layer.

Acknowledgments

We thank Duco I. Hamasaki for discussions and editing the manuscript.

Supported by Grant-in-Aid for Scientific Research C (No. 25462709 [SU]) from the Ministry of Education, Culture, Sports, Science and Technology (http://www.jsps.go.jp/). The authors alone are responsible for the content and writing of the paper.

Disclosure: **N. Hibi**, None; **S. Ueno**, None; **Y. Ito**, None; **C.-H. Piao**, None; **M. Kondo**, None; **H. Terasaki**, None

References

1. McCarty DJ, Mukesh BN, Chikani V, et al. Prevalence and associations of epiretinal membranes in the visual impairment project. *Am J Ophthalmol.* 2005;140:288–294.
2. Aso H, Iijima H, Imai M, Gotoh T. Temporal changes in retinal thickness after removal of the epiretinal membrane. *Acta Ophthalmol.* 2009;87:419–423.
3. Massin P, Allouch C, Haouchine B, et al. Optical coherence tomography of idiopathic macular epiretinal membranes before and after surgery. *Am J Ophthalmol.* 2000;130:732–739.
4. Treumer F, Wacker N, Junge O, Hedderich J, Roider J, Hillenkamp J. Foveal structure and thickness of retinal layers long-term after surgical peeling of idiopathic epiretinal membrane. *Invest Ophthalmol Vis Sci.* 2011;52:744–750.
5. Kim J, Rhee KM, Woo SJ, Yu YS, Chung H, Park KH. Long-term temporal changes of macular thickness and visual outcome after vitrectomy for idiopathic epiretinal membrane. *Am J Ophthalmol.* 2010;150:701–709.
6. Suh MH, Seo JM, Park KH, Yu HG. Associations between macular findings by optical coherence tomography and visual outcomes after epiretinal membrane removal. *Am J Ophthalmol.* 2009;147:473–480.
7. Wilkins JR, Puliafito CA, Hee MR, et al. Characterization of epiretinal membranes using optical coherence tomography. *Ophthalmology.* 1996;103:2142–2151.
8. Arichika S, Hangai M, Yoshimura N. Correlation between thickening of the inner and outer retina and visual acuity in patients with epiretinal membrane. *Retina.* 2010;30:503–508.
9. Kim JH, Kang SW, Kong MG, Ha HS. Assessment of retinal layers and visual rehabilitation after epiretinal membrane removal. *Graefes Arch Clin Exp Ophthalmol.* 2013;251:1055–1064.
10. Lim JW. Results of spectral-domain optical coherence tomography by preferential hyperacuity perimeter in patients after

idiopathic epiretinal membrane surgery. *Curr Eye Res.* 2011; 36:364-369.

11. Okamoto F, Sugiura Y, Okamoto Y, Hiraoka T, Oshika T. Associations between metamorphopsia and foveal microstructure in patients with epiretinal membrane. *Invest Ophthalmol Vis Sci.* 2012;53:6770-6775.
12. Watanabe A, Arimoto S, Nishi O. Correlation between metamorphopsia and epiretinal membrane optical coherence tomography findings. *Ophthalmology.* 2009;116:1788-1793.
13. Lim JW, Cho JH, Kim HK. Assessment of macular function by multifocal electroretinography following epiretinal membrane surgery with internal limiting membrane peeling. *Clin Ophthalmol.* 2010;4:689-694.
14. Moschos M, Apostolopoulos M, Ladas J, et al. Assessment of macular function by multifocal electroretinogram before and after epimacular membrane surgery. *Retina.* 2001;21:590-595.
15. Lai TY, Kwok AK, Au AW, Lam DS. Assessment of macular function by multifocal electroretinography following epiretinal membrane surgery with indocyanine green-assisted internal limiting membrane peeling. *Graefes Arch Clin Exp Ophthalmol.* 2007;245:148-154.
16. Tanikawa A, Horiguchi M, Kondo M, Suzuki S, Terasaki H, Miyake Y. Abnormal focal macular electroretinograms in eyes with idiopathic epimacular membrane. *Am J Ophthalmol.* 1999;127:559-564.
17. Niwa T, Terasaki H, Kondo M, Piao CH, Suzuki T, Miyake Y. Function and morphology of macula before and after removal of idiopathic epiretinal membrane. *Invest Ophthalmol Vis Sci.* 2003;44:1652-1656.
18. Parisi V, Coppe AM, Gallinaro G, Stirpe M. Assessment of macular function by focal electroretinogram and pattern electroretinogram before and after epimacular membrane surgery. *Retina.* 2007;27:312-320.
19. Suzuki T, Terasaki H, Niwa T, Mori M, Kondo M, Miyake Y. Optical coherence tomography and focal macular electroretinogram in eyes with epiretinal membrane and macular pseudohole. *Am J Ophthalmol.* 2003;136:62-67.
20. Terasaki H, Kojima T, Niwa H, et al. Changes in focal macular electroretinograms and foveal thickness after vitrectomy for diabetic macular edema. *Invest Ophthalmol Vis Sci.* 2003;44: 4465-4472.
21. Terasaki H, Ishikawa K, Niwa Y, et al. Changes in focal macular ERGs after macular translocation surgery with 360 degrees retinotomy. *Invest Ophthalmol Vis Sci.* 2004;45:567-573.
22. Sugita T, Kondo M, Piao CH, Ito Y, Terasaki H. Correlation between macular volume and focal macular electroretinogram in patients with retinitis pigmentosa. *Invest Ophthalmol Vis Sci.* 2008;49:3551-3558.
23. Nishihara H, Kondo M, Ishikawa K, et al. Focal macular electroretinograms in eyes with wet-type age-related macular degeneration. *Invest Ophthalmol Vis Sci.* 2008;49:3121-3125.
24. Ishikawa K, Nishihara H, Ozawa S, et al. Focal macular electroretinograms after photodynamic therapy combined with intravitreal bevacizumab. *Graefes Arch Clin Exp Ophthalmol.* 2011;249:273-280.
25. Iwata E, Ueno S, Ishikawa K, et al. Focal macular electroretinograms after intravitreal injections of bevacizumab for age-related macular degeneration. *Invest Ophthalmol Vis Sci.* 2012;53:4185-4190.
26. Srinivasan VJ, Wojtkowski M, Witkin AJ, et al. High-definition and 3-dimensional imaging of macular pathologies with high-speed ultrahigh-resolution optical coherence tomography. *Ophthalmology.* 2006;113:2054-2065.
27. Inoue M, Morita S, Watanabe Y, et al. Inner segment/outer segment junction assessed by spectral-domain optical coherence tomography in patients with idiopathic epiretinal membrane. *Am J Ophthalmol.* 2010;150:834-839.
28. Wojtkowski M, Bajraszewski T, Gorczynska I, et al. Ophthalmic imaging by spectral optical coherence tomography. *Am J Ophthalmol.* 2004;138:412-419.
29. Miyake Y, Shiroyama N, Ota I, Horiguchi M. Oscillatory potentials in electroretinograms of the human macular region. *Invest Ophthalmol Vis Sci.* 1988;29:1631-1635.
30. Miyake Y. Studies of local macular ERG [in Japanese]. *Nippon Ganka Gakkai Zasshi.* 1988;92:1419-1449.
31. Sakai T, Kondo M, Ueno S, Koyasu T, Komeima K, Terasaki H. Supernormal ERG oscillatory potentials in transgenic rabbit with rhodopsin P347L mutation and retinal degeneration. *Invest Ophthalmol Vis Sci.* 2009;50:4402-4409.
32. Kondo M, Ueno S, Piao CH, Miyake Y, Terasaki H. Comparison of focal macular cone ERGs in complete-type congenital stationary night blindness and APB-treated monkeys. *Vision Res.* 2008;48:273-280.
33. Korol S, Leuenberger PM, Englert U, Babel J. In vivo effects of glycine on retinal ultrastructure and averaged electroretinogram. *Brain Res.* 1975;97:235-251.
34. Nakatsuka K, Hamasaki DI. Destruction of the indoleamine-accumulating amacrine cells alters the ERG of rabbits. *Invest Ophthalmol Vis Sci.* 1985;26:1109-1116.
35. Wachtmeister L. Oscillatory potentials in the retina: what do they reveal. *Prog Retin Eye Res.* 1998;17:485-521.
36. Kolb H, Famiglietti EV. Rod and cone pathways in the inner plexiform layer of cat retina. *Science.* 1974;186:47-49.

Investigative Ophthalmology & Visual Science

Int Ophthalmol
DOI 10.1007/s10792-013-9855-y

ORIGINAL PAPER

Transient increase of retinal nerve fiber layer thickness after macular hole surgery

Nobuaki Hibi · Mineo Kondo · Kohei Ishikawa · Shinji Ueno · Keiichi Komeima · Hiroko Terasaki

Received: 27 March 2013 / Accepted: 14 September 2013

Abstract We studied the changes in the thickness of the retinal nerve fiber layer (RNFL) after surgery for idiopathic macular hole (MH) using spectral-domain optical coherence tomography (SD-OCT). Twenty eyes of 20 consecutive patients who underwent vitrectomy to close a MH were studied. The peripapillary RNFL thickness was measured by SD-OCT before and at 1, 3, and 6 months after surgery. The mean overall thickness, the thickness of the four quadrants, and the thickness of each of the 12 clock hours of the RNFL were analyzed. The mean overall RNFL thickness before surgery was 93.3 ± 9.6 μm, and it increased significantly to 98.7 ± 7.4 μm at 1 month after surgery ($P < 0.05$). The mean overall thickness then returned to the pre-surgery level at three and 6 months. The transient increase of RNFL thickness at 1 month after surgery was statistically significant in the superior, nasal, and inferior quadrants. The increase in the thickness of the nasal quadrants was maintained for up to 6 months. When the thickness of the individual 12 clock hours were analyzed, the transient increase of RNFL thickness at 1 month after surgery was significant at each of the 0–5 o'clock positions. The transient increase in the RNFL thickness after MH surgery may be caused by mild edema of the inner retinal layers caused by the MH surgery.

Keywords Macular hole · Retinal nerve fiber layer · Surgery · Optical coherent tomography

N. Hibi · K. Ishikawa · S. Ueno · K. Komeima · H. Terasaki
Department of Ophthalmology, Nagoya University Graduate School of Medicine, Nagoya, Japan

M. Kondo (✉)
Department of Ophthalmology, Mie University Graduate School of Medicine, 2-174 Edobashi, Tsu 514-8507, Japan
e-mail: mineo@clin.medic.mie-u.ac.jp

Published online: 28 September 2013

Background

The rate of an anatomical closure of an idiopathic macular hole (MH) by vitrectomy with internal limiting membrane (ILM) peeling is very high, and the closure is accompanied by significant visual improvements in most cases [1–4]. Although MH surgery has generally been considered to be a safe procedure, various complications have been reported. One of the most serious complications is the development of visual field defects in the peripheral retina [5–10]. The exact mechanism causing the visual field defects after the surgery has still not been definitively determined, but it has been postulated that the defects are caused by inner retinal damage due to air-flow drying during the infusion of air through the canula [11, 12], prolonged gas tamponade [6, 7], or the removal of the posterior hyaloid membrane [6, 7, 9].

We have previously recorded full-field electroretinograms before and after MH surgery [13], and found that the amplitude of the photopic negative

response (PhNR) was significantly reduced after MH surgery even though the patients did not have any visual field defects. However, the amplitude of the photopic a- and b-waves was not significantly altered. Because the PhNR is believed to originate mainly from the electrical activity of ganglion cells and their axons, these results suggested that there may be functional impairments of the inner retina after MH surgery.

These results motivated us to examine the morphological changes of the inner retinal layers before and after MH surgery. Several studies have been published on the morphological changes of the inner retinal layer after MH surgery using scanning laser polarimeter [14] and optical coherence tomography (OCT) [15–18], but the results were very different among these reports.

Thus, the purpose of this study was to investigate the changes in the retinal nerve fiber layer (RNFL) thickness before and after surgery for idiopathic MH. To accomplish this, we examined the retinas by spectral-domain OCT (SD-OCT) before and after MH surgery. We shall show that the mean RNFL thickness increased 1 month after surgery, but then returned to the pre-surgical level at 3 and 6 months after surgery. The possible causes of this transient increase of the RNFL thickness are discussed.

Methods

Subjects

We prospectively studied 20 eyes of 20 consecutive patients (11 male, 9 female) who were scheduled to undergo vitrectomy for an idiopathic MH at the Nagoya University Hospital from March 2009 to September 2010. This study was approved by the Institutional Review Board of the Nagoya University Graduate School of Medicine. All examinations and investigations adhered to the tenets of the Declaration of Helsinki. Informed consent was obtained from each of the patients after an explanation of the procedures to be used and possible complications.

The age of the patients ranged from 44–76 years (mean 63.3 ± 8.4). Patients who were taking glaucoma medications or had visual field defects were excluded. The MH of 10 eyes were at stage 2, eight eyes at stage 3, and two eyes at stage 4 according to the Gass classification [19, 20].

Surgical procedures

Standard three-port pars plana vitrectomy was performed on all eyes either with a 20 gauge system (17 eyes) or 23 gauge system (3 eyes). After a core vitrectomy, triamcinolone acetonide (Kenakolt; Bristol-Myers-Squibb, New York, USA) was injected into the vitreous cavity to make the vitreous gel more visible. A posterior vitreous detachment (PVD) was then created by suction with the vitreous cutter unless a PVD was already present. As much of the vitreous was removed as possible.

The ILM was then grasped with forceps, peeled, and removed. After fluid–air exchange by passive aspiration with a backflush needle, 0.6 ml of 100 % sulfur hexafluoride (SF6) gas was injected into the vitreous cavity. Postoperatively, all patients were asked to maintain a face-down position for about 7 days.

Peripapillary RNFL thickness

SD-OCT was performed with the Cirrus HD-OCT (software version 3.0) (Carl Zeiss Meditec Inc.) before and at 1, 3, and 6 months after MH surgery. The principles of SD-OCT have been described in detail [21]. The scan speed for Cirrus is 27,000 A-scans/sec and the axial resolution is 5 μm. The fast RNFL scan protocol (software version 3.0) was used to measure the peripapillary RNFL thickness. The scan consisted of 256 radial axial scans along a circle with a diameter of 3.46 mm. The center of the scan was manually positioned at the center of the optic disc.

Three types of analysis of the RNFL thickness were made. The first was the average of the RNFL thickness over the entire circumference (256 values) of the optic disc, i.e., the average overall RNFL thickness. The second was the thickness of the RNFL in the four quadrants—superior (46–135°), nasal (136–225°), inferior (226–315°), and temporal (316–45°) quadrants. The third was the RNFL thickness at each of the 12 clock hours. The right eye orientation was used for the clock hour designations. All of the OCT scans had a signal strength ≥7.

Visual acuity and visual fields

The visual acuity was measured before, and at 1, 3, and 6 months after surgery with a standard Japanese visual acuity chart, and the decimal visual acuity was

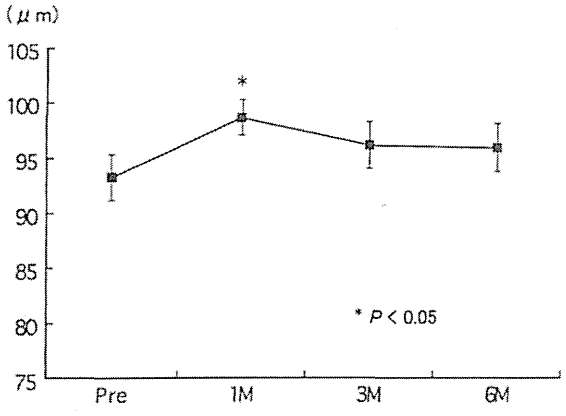

Fig. 1 Changes in the average overall RNFL thickness before and at 1, 3, and 6 months after MH surgery. *Bars* indicate the standard error of the means of 20 eyes; $*P < 0.05$

converted to the logarithm of the minimum angle of resolution (logMAR) units for statistical analyses. We also performed Goldmann perimetry before and at 6 months after surgery (stimulus sizes I2, I3, I4, and V4).

Statistical analyses

The significance of the differences in best-corrected visual acuity (BCVA) and RNFL thickness between pre-operative and post-operative values was determined by the Wilcoxon signed rank test. Differences were considered to be significant when the P value was <0.05.

Results

The MH was closed in all 20 eyes after a single surgery. The BCVA was 0.74 ± 0.24 (mean ± SD) before surgery, and it significantly improved to 0.49 ± 0.19, 0.36 ± 0.23, and 0.30 ± 0.20 at 1, 3, and 6 months after surgery, respectively ($P < 0.05$). None of the eyes had any visual field defects when examined by Goldmann perimetry at 6 months after surgery. In addition, none of the patients had any visual complaints after surgery.

Peripapillary RNFL thickness

The average overall RNFL thickness was 93.3 ± 9.6 μm before surgery, and the thickness increased significantly to 98.7 ± 7.4 μm (5.5 % increase) 1 month after surgery ($P < 0.05$, Fig. 1). The overall thickness then decreased to 96.2 ± 9.7 μm at three and 96.0 ± 10.0 μm at 6 months after surgery. The RNFL thickness at 3 and 6 months after surgery was not significantly different from the preoperative value.

The RNFL thickness in each of the four quadrants was significantly increased at 1 month but then returned to the pre-surgery level at 6 months after surgery in the superior and inferior quadrants (Fig. 2). The RNFL thickness in the nasal quadrant was significantly thicker at 1 month after surgery and remained thicker at 6 months after the surgery. In the temporal quadrant, the RNFL was thicker at 1 month but this increase was not statistically significant. Figure 3 shows representative color maps of the overall and four quadrant RNFL thicknesses before and after surgery for a 60-year-old woman. An increase in the RNFL thickness after surgery can be seen in the nasal, superior and inferior quadrants.

To examine the changes in the RNFL thickness more finely, we analyzed the changes in the RNFL thickness before and after surgery at each of the 12 clock hours (Table 1). At each clock hour between 6 and 11 clock hours, there was no significant difference in the RNFL thickness before and after surgery. On the other hand, the RNFL thickness increased significantly at 1 month after surgery between the 0 and 5 clock hours. At 3 months after surgery, there were five regions (0, 1, 3, 4, and 5 clock hours) where the RNFL was significantly thicker than before surgery. At 6 months after surgery, there were still four regions (0, 1, 3, and 4 clock hours) where the RNFL was significantly thicker than before surgery.

The relative RNFL thicknesses after surgery compared to before surgery are shown in Fig. 4. We found that at 1 month after surgery, the mean relative RNFL thickness increased >10 % at four regions—0, 1, 3, and 4 clock hours. At 3 and 6 months, there were still two regions, 3 and 4 clock hours, where the mean relative RNFL was still thicker by 10 % than before surgery.

Discussion

There are several studies on the morphological changes of the inner retinal layer after MH surgery [14–18]. Ebisawa et al. [14] used scanning laser polarimetry to

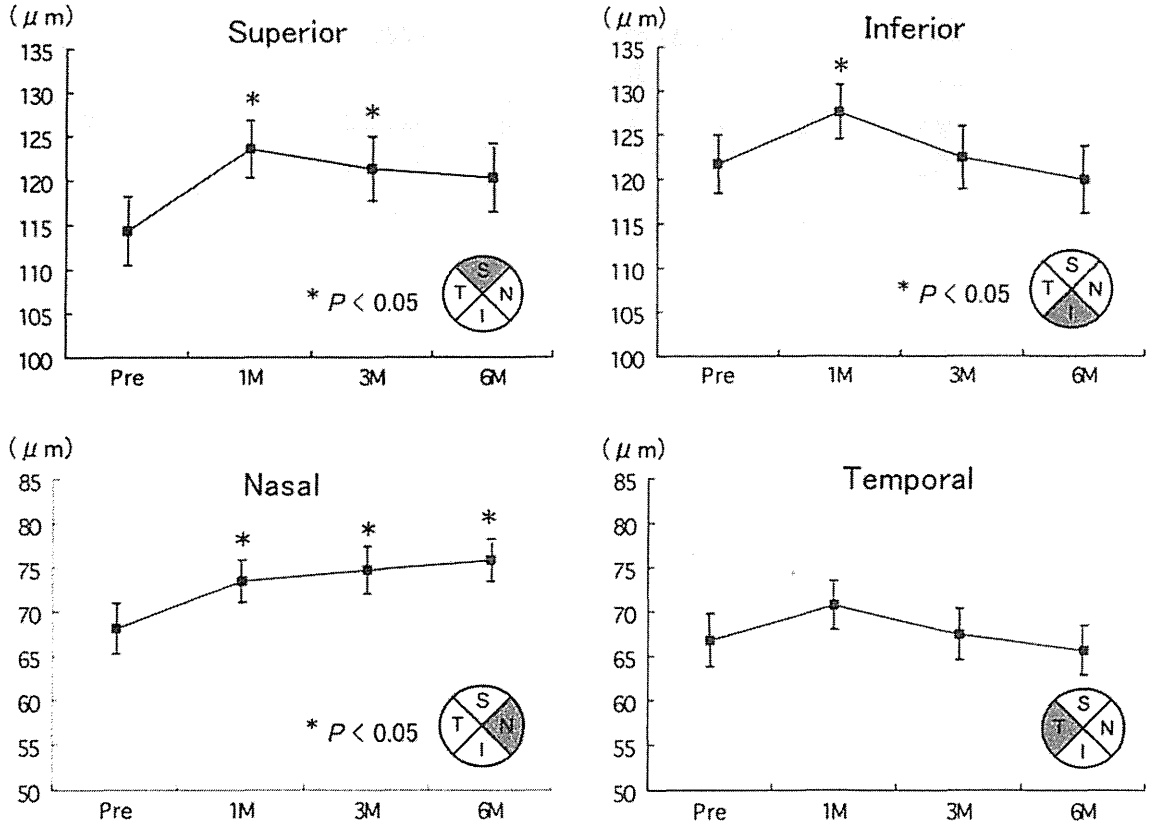

Fig. 2 Changes in the average RNFL thickness in the four quadrants before and at 1, 3, and 6 months after MH surgery. *Bars* indicate the standard error of the means of 20 eyes; $*P < 0.05$

study the changes in the RNFL thickness before and after MH surgery without ILM peeling. They reported that the RNFL thickness decreased significantly up to 3 months after MH surgery, but it then increased up to 12 months to the preoperative thickness. They found that the decrease of RNFL thickness was more severe in cases with visual field defects after surgery, and concluded that the visual field defects were due to inner retinal damage caused by the surgery. In 2006, Yamashita et al. [15] studied the RNFL thickness after MH surgery with ILM peeling using time-domain OCT, and reported that the decrease of RNFL thickness after surgery was more severe in eyes with visual field defects than in eyes without visual field defects. Brazititos et al. [16] also measured the RNFL thickness by time-domain OCT before and at 6 months after Trypan blue-assisted MH surgery with ILM peeling and did not find any significant changes in the overall peripapillary RNFL thickness or in the four quadrants.

The pattern of the changes in the RNFL thickness after MH surgery in our patients was different from these past reports; in our patients, the overall peripapillary RNFL increased significantly 1 month after surgery and then returned to the pre-surgery level 3 months after surgery. A more detailed regional analysis demonstrated that this transient increase of RNFL was significant in the superior, nasal and inferior quadrants especially at the 0–5 clock hours.

Our findings are very similar to those of Tsuiki et al. [17, 18] who investigated the RNFL thickness before and after vitrectomy with ILM peeling in patients with MH using time-domain OCT. They reported that the RNFL thickness increased at about 1 week after surgery, then returned to pre-surgery level. Although the degree of increase in RNFL thickness after surgery was greater in the study by Tsuiki et al. (10.8–12.5 % at average 8.6 days) than in our study (5.5 % at 1 month), the time-course of the changes of the RNFL

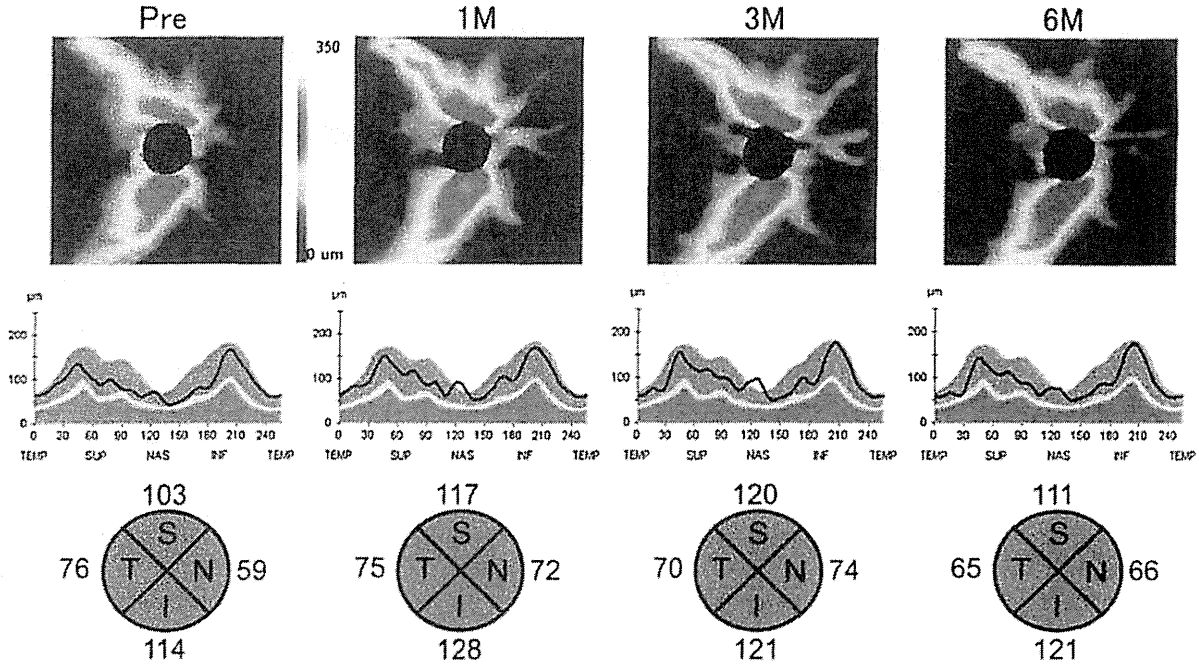

Fig. 3 Color coded maps of the retinal nerve fiber layer (RNFL) thickness (*top panel*), the RNFL thicknesses around the optic disc (*middle panel*), and average RNFL thickness values for the four quadrants of a representative eye before and at 1, 3, and 6 months after surgery. In the RNFL thickness map, false color coding of RNFL thickness with a *scale bar* is displayed. The RNFL thickness increased at the nasal, superior, and inferior quadrants after surgery

Table 1 Changes in the RNFL thickness before and after surgery at 12 clock hour regions

	Pre	1 month	3 months	6 months
0 (superior)	117.2 ± 28.6	129.8 ± 25.2*	128.5 ± 28.1*	125.2 ± 31.0*
1	103.0 ± 21.8	114.0 ± 22.0*	109.6 ± 22.3*	111.1 ± 22.6*
2	81.3 ± 20.0	86.3 ± 18.5*	83.7 ± 13.5	84.8 ± 13.1
3 (nasal)	59.4 ± 12.8	65.6 ± 11.3*	69.1 ± 15.6*	69.5 ± 12.8*
4	61.5 ± 15.4	70.0 ± 12.3*	70.7 ± 15.3*	70.6 ± 14.7*
5	92.7 ± 19.3	99.8 ± 20.5*	97.4 ± 21.3*	96.4 ± 22.2
6 (inferior)	133.7 ± 21.0	138.7 ± 20.3	134.4 ± 22.6	136.5 ± 19.7
7	131.7 ± 34.1	136.7 ± 34.9	131.3 ± 37.7	127.0 ± 37.8
8	70.6 ± 17.4	71.4 ± 14.0	69.0 ± 14.9	67.2 ± 16.9
9 (temporal)	58.4 ± 15.3	58.8 ± 10.1	55.5 ± 11.1	54.2 ± 10.5
10	77.5 ± 19.5	78.7 ± 14.3	75.1 ± 17.8	71.6 ± 16.0
12	119.4 ± 23.1	125.9 ± 21.7	123.1 ± 24.9	120.5 ± 20.8

Right eye orientation was used for documentation of clock hour measurements

* $P < 0.05$

thickness after surgery was very similar to our results. They hypothesized that the transient increase in RNFL thickness after surgery was due to mild edema of the RNFL which was caused by the vitrectomy.

We do not know exactly what procedure of the vitrectomy caused this transient increase in RNFL thickness after MH surgery. There are many papers suggesting that indocyanine green (ICG), which was used to make the ILM more visible, has a toxic effect on the inner retina [22–26]. However, we did not use ICG to stain the ILM during the surgery. If the removal of ILM caused the transient edema of RNFL, the increase of the RNFL thickness should be most prominent in the temporal quadrant. However, our results showed that the transient increase of RNFL was not significant in the temporal quadrant (Fig. 2).